Multi-episode chromospheric evaporation observed in a solar flare

Nai-hwa Chen[1], Hui Tian[2]

[1]National Central University [2]Peking University

High-resolution IRIS observations with spectral lines such Fe XXI 1354.08 Å have revealed new insight into magnetic reconnection, chromospheric evaporation, loop oscillation and other important physical processes during flares. With IRIS observations, here we report multi-episode chromospheric heating and evaporation during an M1.6 flare SOL2015-03-12T11:50. The cool Si IV and Mg II lines reveal quasi-periodically enhanced red wing asymmetries, which are accompanied by episodes of chromospheric evaporation. In the first episode, the Fe XXI 1354 Å line is entirely blueshifted. In the second episode, the Fe XXI line reveals a nearly stationary component and a blueshifted component, which may result from a superposition of the newly evaporated hot plasma on the flare loop that is fillled with hot materials through the first episode of evaporation in the LOS. In both episodes, the blue shift of Fe XXI 1354.08 Å smoothly decreases from ~300 km/s to nearly zero within 3 minutes.

Diagnosing flare dynamics through Fe XXI 1354.08 Å

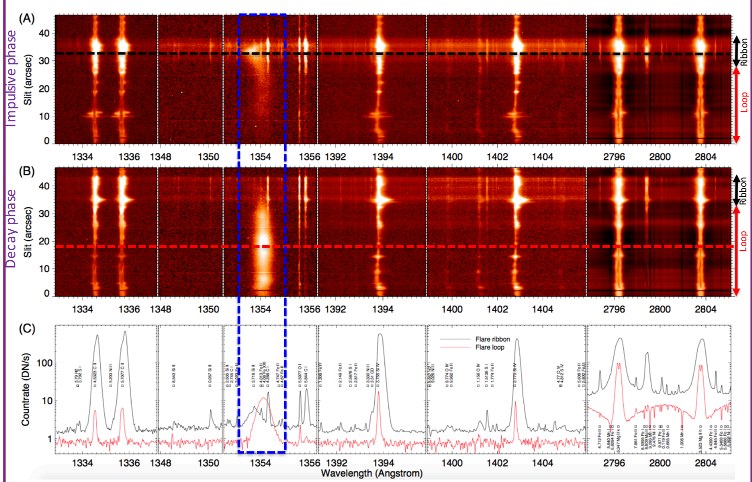

Fig. 1. Typical IRIS spectra in solar flares (Tian et al. 2015).

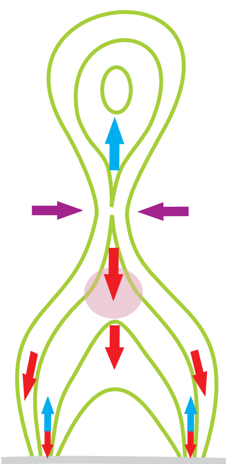

Fig. 2. Different types of flows in the standard flare model.

- Fe XXI is formed at a temperature of ~11 MK and it has been observed in hundreds of flares.
- Above loop top (reconnection downflow):
  (1) Red shift of ~200 km/s, nothermal width ~100 km/s, observed in only a few flares
  (2) References: Tian et al. 2014; Tian & Chen 2018
- Loop footpoints (evaporation flows at or near ribbons):
  (1) Entirely blueshifted by up to ~350 km: flare kernels are resolved by IRIS
  (2) Maximum blue shifts sometimes offset from the ribbons: geometry effect
  (3) Blue shift smoothly decreases to ~0 km/s within a few minutes, and appears to correlated with the energy deposition rate
  (4) References: Tian et al. 2014, 2015; Young et al. 2015; Li et al. 2015; Battaglia et al. 2015; Graham & Cauzzi 2015; Brosius & Daw 2015; Polito et al. 2015, 2016; Sadykov et al. 2016; Zhang et al. 2016; Lee et al. 2017; Li et al. 2017; Brosius & Inglis 2017; Tian & Chen 2018; et al.
- Flare Loops:
  (1) Often strong emission, Zero or small Doppler shift
  (2) Global sausage oscillations with a period of ~25 s detected (Tian et al. 2016)

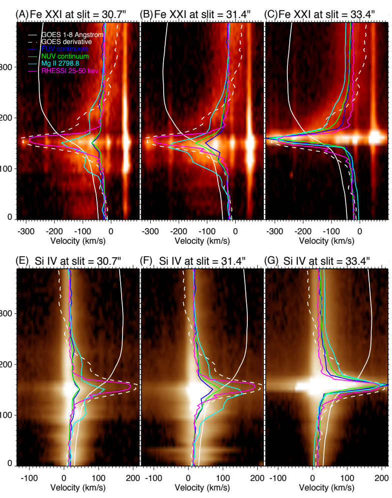

Fig. 3. Temporal evolution of the IRIS spectra in the 1354 Å and 1393 Å windows at a flare ribbon. Fe XXI velocity peaks before SXR peak, correlates with HXR, SXR derivative, UV continuum and Mg II 2798.8 Å intensity, suggesting chromospheric evaporation driven by nonthermal electron (Tian et al. 2015).

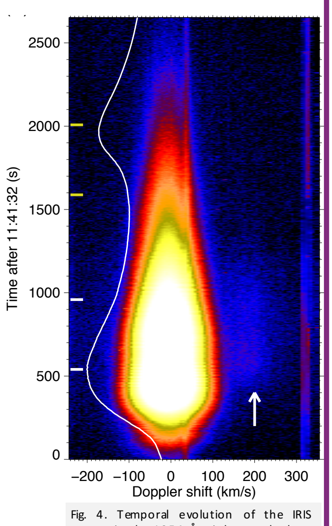

Fig. 4. Temporal evolution of the IRIS spectra in the 1354 Å window at the loop top of a flare. Strong stationary emission from the flare loop and a ~200km/s downflow can be seen (Tian & Chen 2018).

Multi-episode chromospheric evaporation at a flare ribbon

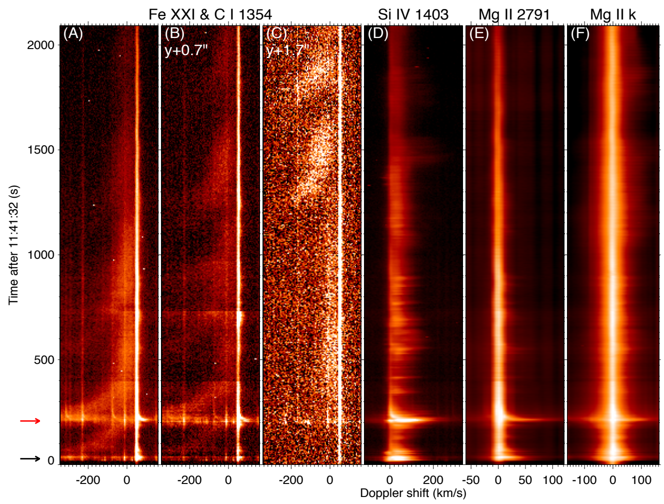

Fig. 5. Temporal evolution of the IRIS spectra in four spectral windows at the northern ribbon of the M1.6 flare SOL2015-03-12T11:50. (B)-(C) are the same as (A) but along two lines that are 0.7" and 1.7" above the ribbon, respectively. The black and red arrows indicate the times of 11:42 UT and 11:45 UT, respectively.

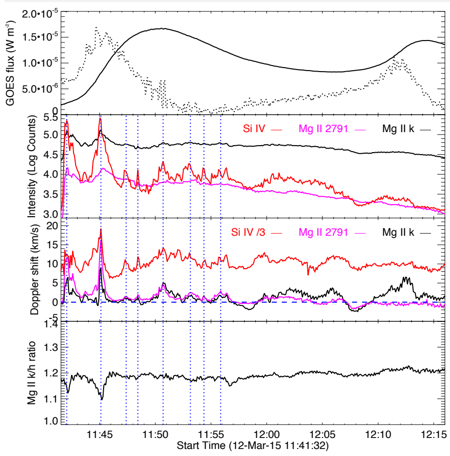

Fig. 6. Upper panel: GOES 1-8 Å flux (solid line) and its time derivative (dotted line). Note that the peak after 12:00 UT is produced by another flare. Lower three panels: Temporal evolution of the intensities and Doppler shifts of Si IV 1402.77 Å, Mg II 2791.59 Å and Mg II k, and the Mg II k/h ratio, at the northern ribbon. The Doppler shift values of the Si IV line have been divided by three. The vertical dotted lines indicate some instants when the red shifts of these lines are enhanced.

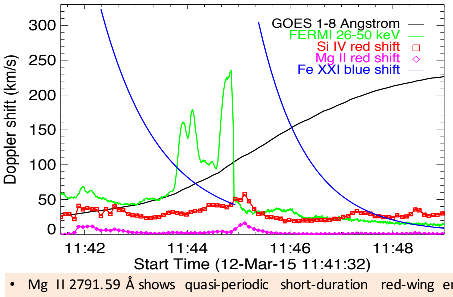

Fig. 7. Time history of the GOES 1-8 Å flux, FERMI 26-50 keV flux, Doppler shifts of Si IV 1402.77 Å, Mg II 2791.59 Å and Fe XXI 1354 Å at the northern ribbon. The GOES and FERMI light curves have been normalized to fit conveniently on this velocity plot.

- Mg II 2791.59 Å shows quasi-periodic short-duration red-wing enhancement, which is likely related to repetitive chromospheric condensation as a result of episodic heating.
- On the contrary, Si IV 1402.77 Å reveals a persistent red-wing asymmetry in both the impulsive and decay phases, suggesting that this line responds to both cooling down flows and chromospheric condensation.
- The first two episodes of red-wing enhancement occurred around 11:42 UT and 11:45 UT, when two moving brightenings indicative of heating fronts crossed the IRIS slit. The greatly enhanced red wings of the Si IV and Mg II lines at these occasions are accompanied by an obvious increase in the line intensities and the HXR flux, suggesting two episodes of energy injection into the lower atmosphere in the form of nonthermal electrons.
- Correspondingly, the Fe XXI 1354 Å line reveals two episodes of chromospheric evaporation, which is characterized as a smooth decrease of the blue shift from ~300 km/s to nearly zero within 3 minutes. The Fe XXI 1354 Å line is entirely blueshifted in the first episode, while appears to contain a nearly stationary component and a blueshifted one in the second episode.
- More episodes of blueshifted Fe XXI emission is found around the northern ribbon in the decay phase, though no obvious response is detected in the Si IV and Mg II emission.

IRIS-9, Göttingen, 25-29 June 2018

Poster

4. Eruptions in the solar atmosphere

Multi-episode Chromospheric Evaporation Observed in a Solar Flare

Chen, N.-H.[1&2], Tian, H.[3]

[1] *Korea Astronomy and Space Science Institute, Republic of Korea*
[2] *Graduate Institute of Astronomy, National Central University, Taiwan*
[3] *School of Earth and Space Sciences, Peking University, Peoples Republic of China*

With observations of IRIS, we study chromospheric heating and evaporation during an M1.6 flare SOL2015-03-12T11:50. At the flare ribbons, the Mg II 2791.59 Å line shows quasi-periodic short-duration red-wing enhancement, which is likely related to repetitive chromospheric condensation as a result of episodic heating. On the contrary, the Si IV 1402.77Å line reveals a persistent red-wing asymmetry in both the impulsive and decay phases, suggesting that this line responds to both cooling downflows and chromospheric condensation. The first two episodes of red-wing enhancement occurred around 11:42 UT and 11:45 UT, when two moving brightenings indicative of heating fronts crossed the IRIS slit. The greatly enhanced red wings of the Si IV and Mg II lines at these occasions are accompanied by an obvious increase in the line intensities and the HXR flux, suggesting two episodes of energy injection into the lower atmosphere in the form of nonthermal electrons. The Mg II k/h ratio has a small value of$\sim$1.2 at the ribbons and decreases to$\sim$1.1 at these two occasions. Correspondingly, the Fe XXI 1354Å line reveals two episodes of chromospheric evaporation, which is characterized as a smooth decrease of the blueshift from$\sim$300 km s^{-1} to nearly zero within$\sim$3 minutes. The Fe XXI 1354Å line is entirely blueshifted in the first episode, while it appears to contain a nearly stationary component and a blueshifted component in the second episode. Additional episodes of blueshifted Fe XXI emission are found around the northern ribbon in the decay phase, though no obvious response is detected in the Si IV and Mg II emission.